

Raman Spectroscopy of Mott insulator states in optical lattices

P. Blair Blakie

*Department of Physics, University of Otago, P.O Box 56, Dunedin, New Zealand.**

(Dated: 26th February 2019)

We propose a Raman spectroscopy technique for probing the properties of quantum degenerate bosons in the ground band of an optical lattice. Our formalism is valid for deep lattices where a tight-binding approach can be applied. We show that in certain limits that shifts in the resonant frequency of excitation reveal the distribution of particles per site and will be a useful tool for characterizing Mott-insulator states produced in experiments.

PACS numbers: 03.75.-b, 03.75.Hh

The observation of the Mott-insulator state of a degenerate Bose gas in an optical lattice [1] has opened an exciting new avenue for investigating strongly correlated condensed matter systems. Ensuing experiments (e.g. [2, 3, 4]) have investigated a wide variety of phenomena making optical lattices one of the leading systems for studying quantum atom optics.

In the initial experimental report, two key pieces of evidence were given for the Mott insulator state: the loss of phase coherence, and the appearance of a gap in the excitation spectrum. However, the original proposal for producing a Mott insulator state by Jaksch et al. [5] predicts a rather complicated Mott insulator phase, arising from the effect of the inhomogeneous trapping potentials that are necessary to confine atoms in the experiment. Their prediction suggests that the Mott phase should exhibit a tiered structure with regions of various integer filled Mott insulating states separated by shells of superfluid. There are currently no practical experimental methods to probe this microscopic structure of the state, though Ref. [4] claims to be able to separate sites with one or two atoms. In this letter we explore a theoretical model of Raman spectroscopy of a Mott insulating state, and show that this technique yields detailed information regarding the filling factor distribution in the system.

I - Formalism The system of interest, which we will refer to as system 1, is a degenerate collection of bosonic atoms populating the lowest vibrational band of an optical lattice well-characterized by the Bose-Hubbard Hamiltonian

$$\hat{H}_1 = \epsilon_0 \sum_j \hat{n}_j - J \sum_{\langle i,j \rangle} \hat{a}_i^\dagger \hat{a}_j + \frac{U_{11} \alpha_w}{2} \sum_j \hat{n}_j (\hat{n}_j - 1), \quad (1)$$

where \hat{a}_j is a bosonic operator that annihilates an atom from the Wannier state $w_j(\mathbf{x})$ centered on lattice site j , with $\hat{n}_j = \hat{a}_j^\dagger \hat{a}_j$ the respective number operator. The quantity J , known as the tunneling matrix element, characterizes the tunneling between lattice sites and is determined from band structure calculations [5, 6]. Interactions between particles are described by the matrix element $\alpha_w \equiv \int d^3\mathbf{x} |w_j(\mathbf{x})|^4$ and the coefficient $U_{11} = 4\pi a_{11} \hbar^2 / m$, where a_{11} is the s-wave scattering length for collisions between atoms in internal state 1. We restrict our attention here to the translationally invariant

system (i.e. neglect the influence of external trapping potentials in addition to the optical lattice), and the constant ϵ_0 characterizes the mid-point energy of the ground band.

In this work, we consider a scheme for probing the properties of system 1, by an internal state changing Raman transition, of the form used in Ref. [7] to output couple an atom laser. This type of coupling is described by an interaction term of the form

$$\hat{V} = \frac{V_p}{2} \theta(t) \sum_j \int d^3\mathbf{x} \hat{\psi}_2^\dagger(\mathbf{x}) \hat{a}_j w_j(\mathbf{x}) e^{i(\mathbf{q}\cdot\mathbf{x} - \omega_0 t)} + \text{H.c.}, \quad (2)$$

where $\hat{\psi}_2^\dagger$ is the field operator for bosonic atoms in the second internal state, and the quantities $\hbar\mathbf{q}$ and $\hbar\omega_0$, specify the momentum and energy transfer of the Raman process respectively. For simplicity we define $\hbar\omega_0$ to be the excess energy transferred over the internal state energy difference. We take the amplitude of the Raman coupling to be of strength V_p beginning at $t = 0$, and of duration T_p . We will assume that the internal states 1 and 2 are different hyperfine ground states for which we can neglect any collisional spin evolution (see [8, 9]).

Our interest lies in the linear response regime, where only a small portion of the atoms are scattered into internal state 2. The evolution of these atoms in internal state 2, which we will refer to as system 2, is described by the Hamiltonian

$$\hat{H}_2 = \int d^3\mathbf{x} \hat{\psi}_2^\dagger(\mathbf{x}) (H_{\text{sp}} + U_{12} \sum_j \hat{n}_j |w_j(\mathbf{x})|^2) \hat{\psi}_2(\mathbf{x}) \quad (3)$$

where $H_{\text{sp}} = p^2/2m + V_{\text{ext}}(\mathbf{x})$ is the single particle Hamiltonian with $V_{\text{ext}}(\mathbf{x})$ the external potential (taken to be the same lattice potential experienced by atoms in system 1), and $U_{12} = 4\pi a_{12} \hbar^2 / m$ characterizes the interactions between particles in systems 1 and 2. Within the validity regime of linear response it is permissible to neglect interactions between atoms in system 2, as their density will remain low.

System 2 is initially in the vacuum state, and the spectroscopic signal to be measured is the number of atoms in system 2 after the Raman pulse. This is a convenient experimental observable as detection techniques can readily distinguish between atoms in different internal states [9]. Additionally when the coupling produces atoms in an excited vibrational band, the excited atoms can be differentiated by their behavior upon expansion from the lattice [10, 11]. The expression for the number of excited atoms, derived using linear response

*Electronic address: bblakie@physics.otago.ac.nz

theory, is

$$\langle \hat{N}_2 \rangle = \frac{\pi V_p^2 T_p}{2\hbar^2} \int_{-\infty}^{+\infty} d\omega R(\mathbf{q}, \omega) \frac{2 \sin^2[(\omega - \omega_0)T_p/2]}{\pi T_p (\omega - \omega_0)^2}, \quad (4)$$

where we have introduced the correlation function

$$R(\mathbf{q}, \omega) = \frac{1}{2\pi} \int dt \int d^3 \mathbf{x} \int d^3 \mathbf{x}' e^{i\mathbf{q}\cdot(\mathbf{x}' - \mathbf{x}) + i\omega t} \times \sum_{ij} w_i^*(\mathbf{x}) w_j(\mathbf{x}') \langle \hat{a}_i^\dagger(t) \hat{\psi}_2(\mathbf{x}, t) \hat{\psi}_2^\dagger(\mathbf{x}', 0) \hat{a}_j(0) \rangle_{\text{Eq.}} \quad (5)$$

where the variable Q represents a trace carried out over the number state basis for the operators $\{\hat{a}_j\}$, i.e. $Q \leftrightarrow |\dots, n_{l-1}^Q, n_l^Q, \dots\rangle$, and $|0_2\rangle$ represents the vacuum state of system 2. The operator $\hat{\psi}_j^Q(\mathbf{x}, t)$ is $\hat{\psi}_2(\mathbf{x})$ evaluated in an interaction picture with respect to the Hamiltonian

$$\hat{H}_j^Q \equiv \int d^3 \mathbf{x} \hat{\psi}_2^\dagger(\mathbf{x}) (H_{\text{sp}} + U_{12} \sum_l (n_l^Q - \delta_{lj}) |w_l(\mathbf{x})|^2) \hat{\psi}_2(\mathbf{x}). \quad (7)$$

We note that in deriving Eq. (6) we have made use of the result

$$e^{i\hat{H}_2 t/\hbar} \hat{\psi}_2(\mathbf{x}) e^{-i\hat{H}_2 t/\hbar} \hat{a}_j(0) |Q\rangle = \hat{a}_j(0) |Q\rangle \hat{\psi}_j^Q(\mathbf{x}, t), \quad (8)$$

where the δ_{lj} term in Eq. (7) arises from commuting \hat{a}_j with $\exp(i\hat{H}_2 t/\hbar)$, and we have made the replacement $\hat{n}_l \rightarrow n_l^Q$ as $|Q\rangle$ are number states.

We refer to \hat{H}_j^Q as the Q -defect Hamiltonian for system 2, as it arises from the removal of a system 1 atom from site j of the number state Q . As the system 1 atoms form an effective potential for those in system 2, the removal of an atom at site j due to the Raman excitation creates a potential hole (i.e. the $n_l^Q - \delta_{lj}$ term in Eq. (7)). This defect plays a key role in the response spectrum as we will demonstrate later. Since \hat{H}_j^Q is a quadratic Hamiltonian it can be diagonalized by numerical methods to obtain its eigenvectors $\{\phi_{jm}^Q(\mathbf{x})\}$ and eigenvalues $\{\hbar\omega_{jm}^Q\}$, i.e. $\hbar\omega_{jm}^Q \phi_{jm}^Q(\mathbf{x}) = \hat{H}_j^Q \phi_{jm}^Q(\mathbf{x})$, where m is the quantum number specifying the state and j labels the defect location. We note that in the limit $U_{12} \rightarrow 0$, the $\hbar\omega_{jm}^Q$ reduce to the Bloch states of H_{sp} and m becomes the quasimomentum and band index. We obtain $\hat{\psi}_j^Q(\mathbf{x}, t) = \sum_m \phi_{jm}^Q(\mathbf{x}) \hat{b}_{jm}^Q e^{-i\omega_{jm}^Q t}$, where \hat{b}_{jm}^Q is a bosonic annihilation operator and arrive at the expression

$$R(\mathbf{q}, \omega) = \frac{1}{2\pi} \int dt e^{i\omega t} \sum_Q \sum_{ijm} c_{ij}^Q(t) A_{mjj}^Q A_{mij}^{Q*} e^{-i\omega_{jm}^Q t}, \quad (9)$$

In this expression the time dependence of the operators is in an interaction picture with respect to unperturbed Hamiltonians $\hat{H}_1 + \hat{H}_2$, and the expectation is taken on the initial equilibrium ensemble.

We will now show how to evaluate the correlation function $R(\mathbf{q}, \omega)$, and how it relates to the properties of the atoms in system 1. We take the initial density matrix to be $\rho = \rho_1 \otimes \rho_2^{\text{vac}}$, where ρ_1 is the degenerate lattice state we are interested in probing and ρ_2^{vac} is the initial vacuum state for system 2. We can then show that without further approximation, $R(\mathbf{q}, \omega)$ can be written in the form

$$R(\mathbf{q}, \omega) = \frac{1}{2\pi} \int dt \int d^3 \mathbf{x} \int d^3 \mathbf{x}' e^{i\mathbf{q}\cdot(\mathbf{x}' - \mathbf{x}) + i\omega t} \sum_{Qij} \langle Q | \hat{a}_i^\dagger(t) \hat{a}_j(0) \rho_1 | Q \rangle \langle 0_2 | \hat{\psi}_j^Q(\mathbf{x}, t) \hat{\psi}_2^\dagger(\mathbf{x}', 0) | 0_2 \rangle w_i^*(\mathbf{x}) w_j(\mathbf{x}'), \quad (6)$$

where we have defined the matrix elements $A_{mij}^Q \equiv \int d^3 \mathbf{x} \phi_{jm}^{Q*}(\mathbf{x}) e^{i\mathbf{q}\cdot\mathbf{x}} w_i(\mathbf{x})$, and the system 1 correlation function $c_{ij}^Q(t) \equiv \langle Q | \hat{a}_i^\dagger(t) \hat{a}_j(0) \rho_1 | Q \rangle$.

Eqs. (6) and (9) represent the key results of this work, and we now briefly comment on the physical process they describe. Fundamentally, $R(\mathbf{q}, \omega)$ characterizes the excitation spectrum of atoms from system 1 into system 2. In the context of ultra-cold gases, a result similar to our starting point [Eq. (4)] has been given by Luxat *et al.* [12] for the case of a harmonically trapped Bose gas (also see [13, 14]). However their treatment neglects interactions between atoms in different hyperfine states and assumes the single particle correlation functions for the atoms in systems 1 and 2 are independent. For the case of atoms in a deep optical lattice these approximations are not tenable. In particular, as we noted previously, the lattice site from which the atom is excited acts as the localizing defect and accounting for correlations between the systems (as we have done in Eq. (6)) is essential.

II - Single Site Limit The limiting case of a single tightly confining harmonic well of frequency ω_{ho} is a useful approximation to a deep lattice in the regime where tunneling between sites can be neglected. This limit shows the main physical features of Raman spectroscopy and provides a useful approximation to the full solution. Assuming that interaction shifts are small compared to the oscillator energy $\hbar\omega_{\text{ho}}$, we may approximate the modes of the system as being harmonic oscillator eigenstates $\{\varphi_m(\mathbf{x})\}$, with respective energies $\{\epsilon_m = \hbar\omega_{\text{ho}}(m + 1/2)\}$. For the single site case our formalism maps according to $w_j(\mathbf{x}) \rightarrow \varphi_0(\mathbf{x})$, $\phi_{jm}^Q(\mathbf{x}) \rightarrow \varphi_m(\mathbf{x})$, $A_{mij}^Q \rightarrow A_m \equiv \int d^3 \mathbf{x} \varphi_m^*(\mathbf{x}) e^{i\mathbf{q}\cdot\mathbf{x}} \varphi_0(\mathbf{x})$, with $\hbar\omega_{jm}^Q \rightarrow \hbar\omega_m^n = \epsilon_m + U_{12}\alpha_0 m(n-1)$ where $\alpha_0 m \equiv \int d^3 \mathbf{x} |\varphi_0(\mathbf{x})|^2 |\varphi_m(\mathbf{x})|^2$. Since the Hamiltonian for system 1 reduces to $\hat{H}_1 \rightarrow \epsilon_0 \hat{n} + U_{11} \alpha_w \hat{n}(\hat{n}-1)/2$ in this limit, we have replaced Q by n and evaluated the correlation function as $c_{ij}^Q(t) \rightarrow c_{ij}^n(t) = n \exp(i[\epsilon_0 + U_{11}\alpha_w(n-1)]t/\hbar)$. Using

Eq. (9) with $\rho_1 = \sum_{nn'} |n\rangle \rho_{nn'} \langle n'|$, we obtain

$$R(\mathbf{q}, \omega) = \sum_n \rho_{nn} n |A_m|^2 \delta(\omega_{\text{res}}(n) - \omega), \quad (10)$$

where $\hbar\omega_{\text{res}}(n) = \epsilon_m - \epsilon_0 + [U_{12}\alpha_{0m} - U_{11}\alpha_w](n-1)$. We have also assumed that the probe only couples to a particular excited state m , with the other states sufficiently far detuned that their contribution is negligible.

Eq. (10) shows that the response of the system is proportional to ρ_{nn} , and most notably, if $[U_{12}\alpha_{0m} - U_{11}\alpha_w] \neq 0$, then the response frequency is linearly dependent on the value of n (i.e. the number of atoms at the site). In this regime the Raman spectrum reveals the number distribution at the site. For the case of ^{87}Rb (the atom of primary interest in bosonic optical lattice experiments) the interactions between the relevant hyperfine states are approximately degenerate (i.e. $U_{11} \approx U_{12}$), so that the difference $\alpha_{0m} - \alpha_w$ will be the primary factor in determining the magnitude of the number dependent shift. As an immediate consequence we note that for the case $U_{11} = U_{12}$ and a Raman pulse coupling to ground vibrational state of system 2, then the spectrum will be independent of n (i.e. for $m = 0$ we have $\alpha_{0m} = \alpha_w$). Therefore to obtain a number dependent spectral response with ^{87}Rb will require scattering into excited vibrational states of system 2.

III - Uniform Mott Insulator We now consider the more general case of a translationally invariant lattice with N_s sites and periodic boundary conditions. We assume that the system is deep in the Mott insulating regime, where $U_{11}\alpha_w \gg J$, and the many-body ground state is well approximated as $|Q_n\rangle = |\dots, n, n, \dots\rangle$ (i.e a definite number of atoms at each site). In calculating the response of the system to the Raman probe according to Eq. (6), the summation over Q reduces to this single state. The next order correction to the translationally Mott state is particle hole states [15], which contribute to the ground state with an amplitude $J/U_{11}\alpha_w \ll 1$, and can be neglected.

To obtain an approximation for the temporal correlation function of system 1 in state $|Q_n\rangle$ we ignore the tunneling term in \hat{H}_1 . This approximation amounts to neglecting particle tunneling between sites in system 1 over the time scale of the Raman probe, and should be a good approximation in deep lattices. In this limit the correlation function is $c_{ij}^{Q_n}(t) = n \exp(i[\epsilon_0 + U_{11}\alpha_w(n-1)]t/\hbar)\delta_{ij}$, and making use of the translational invariance in evaluating Eq. (9) we obtain

$$R(\mathbf{q}, \omega) = \sum_m n N_s |A_{ml}^{Q_n}|^2 \delta(\omega - \omega_{\text{res}}^{Q_n m}), \quad (11)$$

where $\omega_{\text{res}}^{Q_n m} = \omega_{lm}^{Q_n} - [\epsilon_0 + U_{11}\alpha_w(n-1)]/\hbar$. Note that due to translational invariance the precise value of l used in Eq. (11) is unimportant. We now calculate the response spectrum $\langle \hat{N}_2 \rangle$ using Eqs. (4) and (11) for a translationally invariant 1D lattice. We take the lattice potential to be $V_{\text{ext}}(x) = V_D \cos^2(x/\lambda)$, arising from counter-propagating lasers fields of wavelength λ , and we specify the lattice depth V_D in units of $E_R = \hbar^2/2m\lambda^2$. The calculation is performed

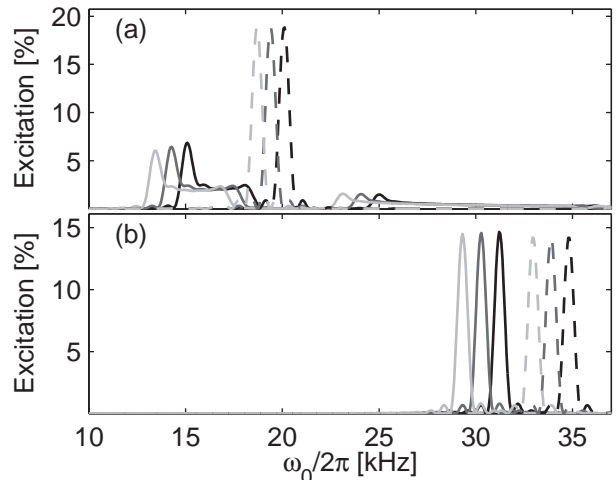


Figure 1: The percentage of atoms excited after Raman excitation in a 1D lattice of depth (a) $V_D = 10E_R$ (b) $V_D = 30E_R$. In each plot the spectrum of Mott insulator states with filling factors of $n = 1$ (dark line), $n = 2$ (medium line) and $n = 3$ (light line) are shown. The respective single site results for $m = 1$ are given as dashed lines. Parameters are $q = \pi/\lambda$, $T_p = 1.5\text{ms}$, $V_p = 0.05E_R$, $\lambda = 850\text{nm}$, $N_s = 51$, transverse confinement taken to be harmonic with $f_{\perp} \approx 7\text{kHz}$, and $a_{11} = a_{12} = 5.29\text{nm}$.

for typical ^{87}Rb parameters (e.g. see Ref. [1]) to demonstrate the practicality of our probing scheme. We will not consider the influence of \mathbf{q} on the spectrum in this paper [16], and for simplicity we have taken \mathbf{q} as being identical to a reciprocal lattice for our calculations.

The results we have obtained are shown in Fig. 1. For the case of $V_D = 10E_R$ (Fig. 1(a)) the Raman response is shown over a frequency range that includes resonant coupling to the first two excited bands. The superimposed graphs show the spectra for Mott insulating states of various filling factors and clearly exhibit frequency shifts proportional to n . Additionally, we notice that in the first excited band (12kHz - 18kHz), the dominant response peak occurs at the low end of the spectral feature (e.g. the peak at $\sim 15.5\text{kHz}$ for $n = 1$), adjacent to a broad base. This feature is also seen in the 2nd excited band (24kHz - 36kHz), however the peaked feature is much less dominant relative to the broad base. The peak originates from an excited band state that is partially localized above the defect site. This localization leads to a strong coupling matrix element $A_{ml}^{Q_n}$, and as this state resides at the defect, its energy is lower than the other states in the excited band. We refer to this state as the defect state, which is clearly identified as the most strongly excited feature at the bottom each band. Since the localization is not perfect, the other states in the excited band have appreciable amplitude at the defect site. These states give rise to the broad though more weakly excited, band of states above the resonant peak. In the 2nd excited band, the same features are seen, however as the effective tunneling in this band is much higher, and the defect state is much less localized.

In Fig. 1(b) the response spectrum is shown for a lattice of depth $V_D = 30E_R$. At this depth the response from the first

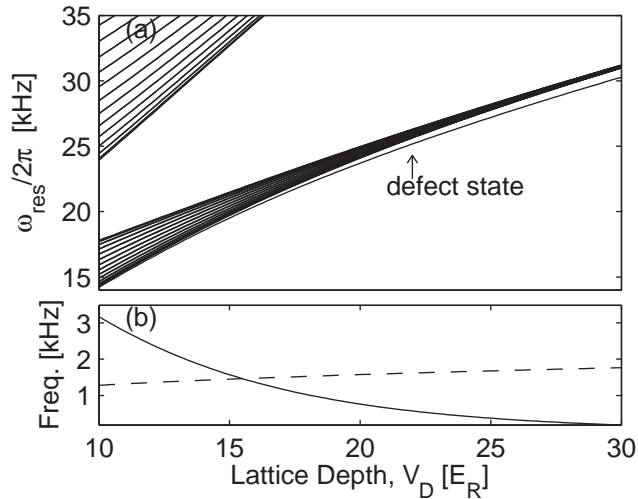


Figure 2: (a) Spectrum of excited states versus lattice depth. (b) The bandwidth of the first excited band (solid) and the on-site interaction (dashed) versus lattice depth. Other parameters as in Fig. 1.

excited band states have shifted up to 30kHz, and the second excited band has moved out of the frequency range considered. In contrast to the spectrum in Fig. 1(a), we only notice the resonant peak due to the defect state, without a discernible broad base of band states. This arises because at this depth the tunneling rate in the excited band is sufficiently small that the defect state becomes completely localized. The other states in the excited band are necessarily orthogonal to the defect state and so have vanishing coupling matrix elements $A_{ml}^{Q_0}$.

For comparison in Figs. 1(a) and (b) we also show the single site predictions for the spectrum calculated using expression (10) with ω_{ho} chosen to match the effective trap frequency at the lattice site minima. The frequency location of the response spectra compares badly with the full lattice solution, arising primarily from the inadequacy of the harmonic approximation for accurately predicting band structure. The location of the spectra can be easily corrected for by calcu-

lating the term $\epsilon_m - \epsilon_0$ in the expression for $\omega_{\text{res}}(n)$ using the non-interacting band structure result. However, the single site approximation captures many of the salient features of the full lattice solution, such as the magnitude of the n -dependent shift in the response spectrum. In the strongly-localized defect limit (Fig. 1(b)), the single site approximation quantitatively predicts the response amplitude as the role of the band states can be neglected.

To quantify the emergence of the defect state we examine the spectrum of $\omega_{\text{res}}^{Q_n m}$ as a function of V_D in Fig. 2(a). For $V_D \gtrsim 15E_R$ a single defect state is observed to drop below the first excited band. The condition for the emergence of a strongly localized defect state is that the energy reduction from localization above the defect in system 1 is large compared to the effective inter-site tunneling in the excited band. To verify this criterion we compare the excited bandwidth (characterizing the excited band tunneling rate) and energy reduction at the defect, approximated by $U_{11}\alpha_w$. These two energy scales are seen to cross at $V_D \approx 15E_R$. Finally, we note the validity condition for linear response treatment of Raman spectroscopy. This requires the number of atoms excited to remain small compared to the total number of atoms in the system. In terms of the Raman parameters this condition is given as $nV_p^2T_p^2/4\hbar^2 \ll 1$, where n is the average number of atoms per site.

While we have only considered the case of a perfect Mott insulator in a translationally invariant lattice, our results suggest that in the limit of strongly localized defect states the response of the system is well-described by the single site result, and thus only depends on the local number distribution at each lattice site. The Raman spectrum can therefore be used to obtain the relative portion of system 1 at sites with filling factor n atoms. Future work will look in more detail at the role of the external confining potential, superfluid regions and thermal excitation in the response of the system.

Acknowledgments PBB would like to acknowledge valuable discussions with Trey Porto, Crispin Gardiner, and thanks the University of Otago for supporting this research.

-
- [1] M. Greiner, O. Mandel, T. Esslinger, T. W. Hänsch, and I. Bloch, *Nature* **415**, 39 (2002).
 - [2] M. Greiner, O. Mandel, T. W. Hänsch, and I. Bloch, *Nature* **419**, 51 (2002).
 - [3] O. Mandel, M. Greiner, A. Widera, T. Rom, T. W. Hänsch, and I. Bloch, *Phys. Rev. Lett.* **91**, 010407 (2003).
 - [4] A. Widera, O. Mandel, M. Greiner, S. Kreim, T. W. Hänsch, and I. Bloch, *Phys. Rev. Lett.* **92**, 1604064 (2004).
 - [5] D. Jaksch, C. Bruder, J. I. Cirac, C. Gardiner, and P. Zoller, *Phys. Rev. Lett.* **81**, 3108 (1998).
 - [6] P. B. Blakie and C. W. Clark, *J. Phys. B* **37**, 1391 (2004).
 - [7] E. Hagley, L. Deng, M. Kozuma, J. Wen, K. Helmerson, S. Rolston, and W. Phillips, *Science* **283**, 1706 (1999).
 - [8] A. Widera, F. Gerbier, S. Fölling, T. Gericke, O. Mandel, and I. Bloch, *Coherent collisional spin dynamics in optical lattices* (2004).
 - [9] D. S. Hall, M. R. Matthews, J. R. Ensher, C. E. Wieman, and E. A. Cornell, *Phys. Rev. Lett.* **81**, 1539 (1998).
 - [10] M. Greiner, I. Bloch, O. Mandel, T. W. Hänsch, and T. Esslinger, *Phys. Rev. Lett.* **87**, 160405 (2001).
 - [11] J. H. Denschlag, J. E. Simsarian, H. Häffner, C. McKenzie, A. Browaeys, D. Cho, K. Helmerson, S. L. Rolston, and W. D. Phillips, *J. Phys. B* **35**, 3095 (2002).
 - [12] D. L. Luxat and A. Griffin, *Phys. Rev. A* **65**, 043618 (2002).
 - [13] S. Choi, Y. Japha, and K. Burnett, *Phys. Rev. A* **61**, 063606 (2000).
 - [14] M. D. Girardeau and E. M. Wright, *Phys. Rev. Lett.* **87**, 050403 (2001).
 - [15] A.-M. Rey, P. B. Blakie, G. Pupillo, C. J. Williams, and C. W. Clark, *Phys. Rev. A* **72**, 023407 (2005).
 - [16] Generally large q favors coupling to higher bands, though certain choices of \mathbf{q} can suppress coupling efficiency, e.g for

$\mathbf{q} = \mathbf{0}$ the response from the first band is zero by symmetry.